FTIR AND WAXS STUDIES ON SIX VEGETAL FIBERS

RANJITHA KEMPAIAH,[*] GAYATHRI GURAPPA,[*] RITU TOMAR,[*]
MATHEUS POLETTO,[**] HEITOR LUIZ ORNAGHI JUNIOR,[**] VENKATASAMY ANNADURAI[*] and
RUDRAPPA SOMASHEKAR[***]

[*]*Department of Physics and Research Centre, Sambhram Institute of Technology,*
Bangalore 560 097, India
[**]*LPOL, University of Caxias do Sul (UCS), Francisco Getúlio Vargas 1130, Caxias do Sul,*
Rio Grande do Sul 95070-560, Brazil
[***]*Regional Institute of Engineering and Department of Studies in Physics,*
University of Mysore, Manasagangotri, Mysore 570 006, India
✉ *Corresponding author: R. Kempaiah, ranjithak.physics@gmail.com*

The microstructural parameters of various vegetal fibers and their respective native cellulose have been studied using wide angle X-ray scattering (WAXS) and FT-IR spectroscopy. The crystal imperfection parameters, such as crystal size $\langle N \rangle$, lattice strain (g) and enthalpy (α^*), have been determined by profile analysis using Warren's method. The results were cross-checked with those obtained by matching the stimulated intensity profile obtained from one-dimensional Hosemann's paracrystalline model. In all this computation, we have used (110) and (200) reflection observed in these varieties of vegetal fibers and their native cellulose. We have also computed volume weighted and surface weighted crystal size, and compared the values of these parameters. Details of the microstructural parameters were obtained using an analytical function considering asymmetric functions, and the variations found in crystallite shape and size were attributed to differences in the chemical composition of lignin and cellulose among the fibers.

Keywords: vegetal fibers, cellulose, WAXS, crystal imperfection parameter, volume weighted crystal size, surface weighted crystal size, FTIR

INTRODUCTION

The last few decades have revealed a growing interest in the research and development of polymeric and composite materials from renewable sources.[1-7] As the most abundant component in most plants, cellulose is an almost inexhaustible polymeric raw material from renewable sources. Natural cellulose-based materials, such as vegetal fibers, have been used as engineering materials for thousands of years and are still used currently, as demonstrated by the huge number of forest product-based industries worldwide. However, what makes cellulose such an important material for the development of polymeric and composite materials? The cellulose macromolecule is made up of repeating glucose units that generate surprising specificity and impressively diverse architectures, reactivates and functions.[8] The reactions and properties of native cellulose are determined by the isolation process used, the number of inter and intra-molecular hydrogen bonds, the chain lengths, chain length distribution, crystallinity and the distribution of functional groups within the repeating units and along the polymer chains.[8-11] These important parameters make cellulose a unique material.

Cellulose is a natural polymer consisting of ringed glucose molecules. The repeat unit comprises two anhydroglucose rings $(C_6H_{10}O_5)_n$ linked together through an oxygen covalently bonded to the C_1 of one glucose ring and the C_4 of the adjoining ring ($1 \rightarrow 4$ linkage), the so-called β-1,4 glucosidic bond.[8,12-14] The degree of polymerization, *n*, varies between 10,000 and 15,000, where *n* is dependent on the cellulose source material.[12,15] Each repeating unit contains three hydroxyl groups, these hydroxyl groups with their ability to make hydrogen bonds between cellulose chains, govern the physical properties of cellulose.[15]

The intra-chain hydrogen bonding between the hydroxyl groups and the oxygen of the adjoining ring molecules stabilizes the linkage and results in the linear configuration of the cellulose chain.[12] During cellulose formation, van der Waals and intermolecular hydrogen bonds between the hydroxyl groups and the oxygen of adjacent molecules promotes aggregation of multiple cellulose chains forming fibrils.[8,12] The intra- and inter-chain hydrogen bonding network makes cellulose a relatively stable polymer, and gives the cellulose fibrils high axial stiffness.[12] The high cohesive energy ensuing from these physico-chemical interactions explains why cellulose does not possess a liquid state[16] and these cellulose fibrils are the main reinforcement phase in trees and plants. Within these cellulose fibrils, there are regions where the cellulose chains are arranged in a highly ordered crystalline structure and regions with a low level of order or amorphous regions.[12,15]

The polymorphy of cellulose and its derivatives has been well documented. These are cellulose I, II, III and IV.[8,11,17] Cellulose I, or native cellulose, is the form found in nature. Its structure is thermodynamically metastable and can be converted to either cellulose II or III.[12,15] This work focuses on the characterization of the cellulose I structure, which is the crystal structure naturally produced by a variety of organisms. Cellulose I has two polymorphs, a monoclinic structure I_β and a triclinic structure I_α, which coexist in various proportions depending on the cellulose structure.[12,18] The I_α is a rare form, whereas I_β is the dominant polymorph for higher plants.[14,19] The I_α polymorph is metastable and can be converted into I_β by hydrothermal treatments in alkaline solution.[12,19]

In the I_α and I_β polymorph structures, the I_α unit cell contains one cellulose chain, the unit cell parameters being a = 0.672 nm, b = 0.596 nm, c = 1.040 nm, α = 118.08°, β = 114.80°, γ = 80.375°.[15] The I_β unit cell contains two cellulose chains, and the unit cell parameters are a = 0.778 nm, b = 0.820 nm, c = 1.038 nm and γ = 96.5°.[19,20] Three lattice planes with approximate d-spacings of 0.39 nm, 0.53 nm and 0.61 nm correspond to the I_α lattice planes (110), (010) and (100) for the triclinic structure, and to the I_β lattice planes (200), (100), and (1-10) for the monoclinic structure.[12,19] The main difference between the I_α and I_β polymorph structures is the relative displacement of cellulose sheets along the (110)

lattice plane in the triclinic structure and the (200) lattice plane in the monoclinic structure, called "hydrogen-bonded" planes, in the chain axis direction.[8,12] In I_α, there is a relative displacement of c/4 between each subsequent hydrogen-bonded plane, while for I_β, the displacement alternates between ±c/4 through van der Waals interactions.[12,19-22]

Therefore, knowledge of the properties of native cellulose before using it in composites can contribute to the development of composites with better mechanical properties.[23] In order to better understand the relationships between native cellulose structure and properties, the aim of this work was to establish the structural differences among some varieties of vegetal fibers, namely kenaf, jute, sisal, curaua, ramie and buriti, commonly used as reinforcing fillers in composite materials. To achieve this objective, FTIR spectroscopy and X-ray diffraction (XRD) analysis were used.

Theory

The intensity of a profile in the direction joining the origin to the center of the reflection can be expanded in terms of Fourier Cosine series:[24-26]

$$I(s) = \sum_{n=-\infty}^{\infty} A(n) \cos\{2\pi nd(s - s_o)\} \tag{1}$$

where the coefficients of the harmonics *A(n)* are functions of the crystallite size and the disorder of the lattice. Here, *s* is (sin θ)/λ and *d* is the lattice spacing. The Fourier coefficients[27-32] can be expressed as:

$$A(n) = A_s(n).A_d(n) \tag{2}$$

For a paracrystalline material, such as vegetal fiber, $A_d(n)$ turns out to be:[26,33]

$$A_d(n) = \exp(-2\pi^2 m^2 n g^2) \tag{3}$$

where *m* is the order of reflection and *g(=Δd/d)* is the lattice strain. For a probability distribution of column lengths *P(i)*, we have:

$$A_s(n) = 1 - \frac{nd}{D} - \frac{d}{D}\left[\int_0^n iP(i)di - n\int_0^n P(i)di\right] \tag{4}$$

where D = <N>d_{hkl} is the crystallite size. In the presence of two orders of reflections from the set of Bragg planes, Warren and Averbach (1952) developed a method of obtaining the crystal size (<N>) and lattice strain (g). However, in wood fibers, multiple reflections are very rarely found. So, to find the finer details of the microstructure, we approximate the size profiles by a simple analytical function for P(i). Here, we have

considered only asymmetric functions. In this way, we can still complete the microstructure parameters by a single order method.

Exponential distribution

It is assumed that there are no columns containing fewer than p units and those with more decay exponentially. Thus we have:[34]

$$P(i) = \begin{cases} 0 & \text{if } p < i \\ \alpha \exp\{-\alpha(i - p)\} & \text{if } p \geq i \end{cases} \quad (5)$$

where $\alpha = (1/(N-p))$. Substituting Equation (5) in Equation (4), we obtain equation (6):

$$A_s(n) = \begin{cases} A(0)\left(1 - \dfrac{n}{\langle N \rangle}\right) & \text{if } n \leq p \\ A(0)\exp\{-\alpha(n - p)\}/(\alpha N) & \text{if } n \geq p \end{cases}$$

Surface and volume weighted crystal sizes

The surface weighted and volume weighted values are computed using a well-established procedure using the parameters $<N>$ and α or β. The relations are given by:[33]

$$D_{v,s} = \frac{\int_0^\infty L P_{v,s}(L)\,dL}{\int_0^\infty P_{v,s}(L)\,dL} \quad (7)$$

where $P_{v,s}(L)$ is the appropriate crystal size distribution functions and $L = n\,d_{hkl}$. Here, n is the harmonic number.[35]

EXPERIMENTAL
Materials

The varieties of vegetal fiber samples used in this study were as follows: *Hibiscus cannabinus* (kenaf), *Corchorus capsularis* (jute), *Agave sisalana* (sisal), *Ananus erectifolius* (curaua), *Boehmeria nivea* (ramie) and *Mauritia flexuosa* (buriti). Kenaf, jute and sisal fibers were supplied by Tapetes São Carlos Technology from São Carlos, Brazil, as sheets. Curaua fiber was obtained from CEAPAC, a support center for community action projects in Santarem, Brazil. Ramie roving was purchased from Sisalsul Fibras Naturais from São Paulo, Brazil, and buriti fiber was obtained from Sisalsul Fibras Naturais from Caxias do Sul, Brazil. All of the fiber samples were dried at 105 °C for 24 h in a vacuum oven before the tests. The samples were ground in a knife mill and the average fiber particle length used in all analyses was around 200 μm.[36] More information about fiber characterization can be found in earlier publications.[6,37]

FT-IR spectroscopy

Fourier transform infrared spectroscopy analysis was carried out on FTIR Nicolet IS10 Thermo Scientific equipment, using 32 scans, in the range of 4000-400 cm^{-1} at a resolution of 4 cm^{-1}. KBr pellets (5 mg of sample for 100 mg of KBr) were prepared. Three measurements were made for each sample and the average value was considered.

X-ray diffraction patterns

The powdered samples were compression moulded under a pressure of 5 tons for 2 min to obtain pellets before XRD analysis. X-ray diffractograms were collected using a sample holder mounted on an XRD 6000 Diffractometer (Shimadzu, Kyoto, Japan), with monochromatic CuKα radiations ($\lambda = 0.15419$ nm). The generator was utilized at 40 kV and 30 mA, and the intensities were measured in the range of $5° < 2\theta < 40°$, typically with scan steps of $0.05°$ at $1.5°$/min (2 s/step). Peak separations were carried out using Gaussian deconvolution. X-ray diffraction patterns of various vegetal fibers and their native cellulose are given in Figure 1 (a-f).

Determination of Fourier coefficients and instrumental broadening corrections

The profile of a Bragg reflection was assumed to be symmetric and the half that had the greatest range before the intrusion of other reflections was used. The background level was taken as that at which intensity either begins to increase with a distance from the peak or becomes uniform. This was subtracted from all the points and the intensity was assumed to be zero over the rest of the range required by the theory. The scattering angle was transformed to $s = \sin\theta/\lambda$ and the values of intensity were interpolated at equal intervals of s of 0.001Å^{-1}, after which they were corrected for Lorentz and polarization factors.

Fourier coefficients were determined using a program written in FTN77 language, and these were again used to predict the intensity data, so that the difference between the predicted and the experimental data is less than 1% of the mean value. Normally, the number of coefficients is of 20-30, which satisfied the condition.[38] Instrumental broadening corrections were applied. For this purpose, standard X-ray profiles at appropriate 2θ angles of the samples were obtained from standard samples, such as ball milled iron powder, and were used for subtracting the instrumental broadening by the Stokes deconvolution method. These corrections are relatively small in polymeric samples when compared to metal oxide compounds.[33,39] We have extensively checked the reliability of this single order method of obtaining the strain parameters in our earlier papers, using man-made polymer samples and employing both multiple and single order methods.[33,34,40]

RESULTS AND DISCUSSION

The FT-IR spectra for the vegetal fibers studied are shown in Figure 2. It can be observed that there is a strong broad band around 3400 cm[-]

[1], which is assigned to different O-H stretching modes,[41] and two bands around 2920 cm^{-1} and 2850 cm^{-1}, related to asymmetric and symmetric methyl and methylene stretching groups, which are notably present in the spectra for cellulose.[5,42] However, these two bands are more prominent at 2918 cm^{-1} and 2849 cm^{-1}, respectively, for buriti fiber. This might be attributed to the higher extractive contents in this fiber, comprising organic extractives, such as fatty acid, methyl, esters and phenolic acid. Methyl esters contain methyl and methylene groups.[42-45] In the fingerprint region, the bands at 1595 cm^{-1}, 1510 cm^{-1} and 1270 cm^{-1} are assigned to C=C, C-O stretching and bending vibrations different groups present in lignin.[5,42-45] The bands at 1460 cm^{-1}, 1425 cm^{-1}, 1335 cm^{-1}, 1220 cm^{-1} and 1110 cm^{-1} are characteristic of C-H, C-O deformation, bending or stretching vibrations of many groups in lignin and carbohydrates.[36,42-45] The bands at 1735 cm^{-1}, 1375 cm^{-1}, 1240 cm^{-1}, 1165 cm^{-1}, 1060 cm^{-1} and 1030 cm^{-1} are assigned to C=O, C-H, C-O-C and C-O deformation or stretching vibrations of different groups in carbohydrates.[5,42,43]
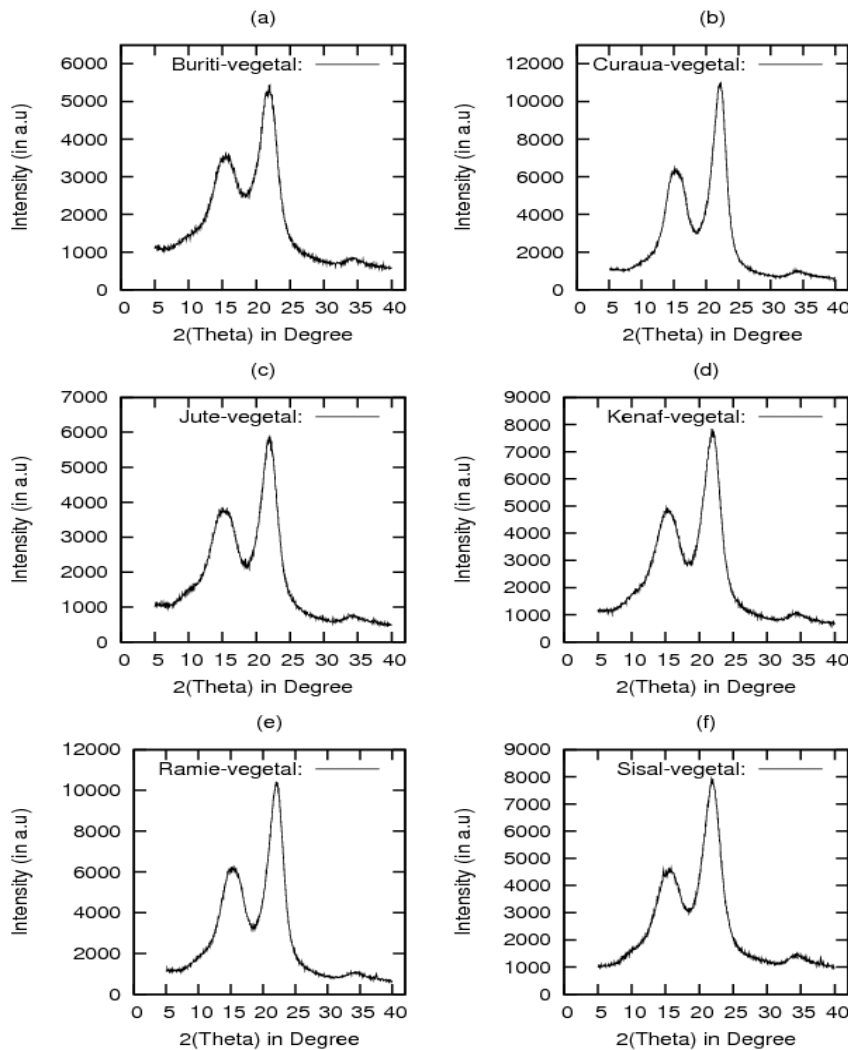

Figure 1: X-ray diffractograms for a) buriti, b) curaua, c) jute, d) kenaf, e) ramie and f) sisal vegetal fibers

The hydrogen bonds are considered to be responsible for various properties of native cellulose lignin and natural fibers. Thus, the closer the cellulose chains, the greater the interaction between the adjacent chains, resulting in more and stronger hydrogen bonds, which can lead to greater packing of cellulose chains, resulting normally in fibers with higher

mechanical and thermal properties.[5,46] In addition, an intra-molecular hydrogen bond vibration for cellulose appears at around 3432 cm^{-1}.[47,48]

According to other studies,[46-49] the intra-molecular hydrogen bond in a phenolic group in lignin is observed at around 3568-3577 cm^{-1}.[36,49] In cellulose, the intra-molecular hydrogen bond vibration appears at around 3432 cm^{-1},[36,47,48] another intra-molecular hydrogen bond in cellulose normally occurs at 3342 cm^{-1}.[48] The two characteristic bands assigned to the two crystalline cellulose allomorphs, cellulose I_α and cellulose I_β, also occur in the region of 3220-3280 cm^{-1}.[42,46] A very small peak, normally shifting to lower wavenumbers at 3221 cm^{-1}, is attributed to hydrogen bonds only in cellulose I_α.[36,42,46,47] The band at 3221 cm^{-1} is assigned to the intra-molecular hydrogen bonds present only in

triclinic I_α cellulose, whereas the band close to 3277 cm^{-1} is proportional to the amount of monoclinic cellulose I_β.

The energy of hydrogen bonds E_H for several OH stretching bonds has been calculated using the equation $E_H = \frac{1}{k}\left(\frac{\gamma_o - \gamma}{\gamma_o}\right)$, where γ_o is the standard frequency corresponding to free OH groups (3560 cm^{-1}), γ is the frequency of bonded OH groups and k is a constant ($1/k = 2.625 \times 10^2$ kJ).[50]

The hydrogen bond distances R are obtained using the equation $\gamma = 4430 \times (2.84 - R)$ cm[-1], where $\Delta\gamma = \gamma_o - \gamma$, γ_o is the monomeric OH stretching frequency, which is taken to be 3600 cm^{-1}, and γ is the stretching frequency observed in the infrared spectrum of the sample.[51]
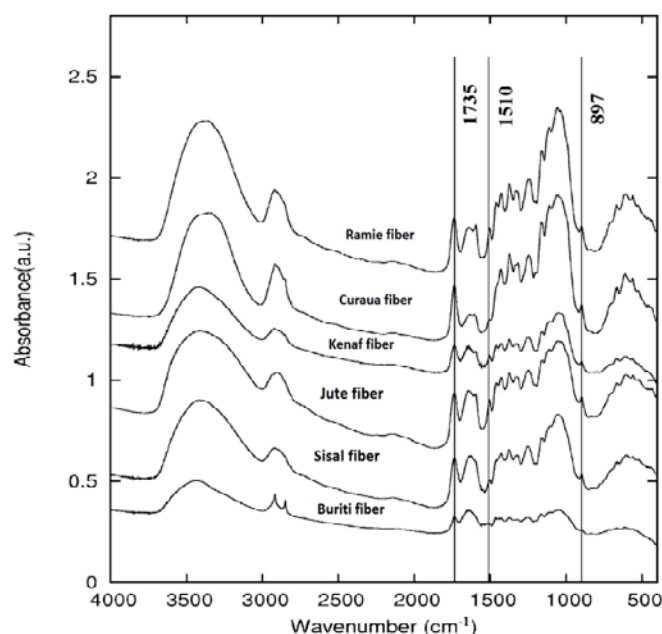

Figure 2: FTIR spectra of buriti, sisal, jute , kenaf , curaua and ramie and vegetal fibers

Table 1
Chemical composition of the vegetal fibers used in this study

Fibers	Cellulose (wt%)	Hemicelluloses (wt%)	Lignin (wt%)	Pectin (wt%)	Waxes (wt%)	Extractives (wt%)
Curaua	71-74	9.9-21	7.5-11	-	0.79-0.9	2.5-2.8
Jute	45-71	13.6-21	12-26	0.2-10	0.5	2
Kenaf	31-72	20.3-23	9-19	3-5	-	2-5
Ramie	68.6-91	5-16.7	0.6-0.7	1.9-2	0.3	6
Sisal	65-67	12	9.9	2-10	0.3-2	0.8-2
Buriti	47-63	4-26.6	21-27	-	-	5.4-6.0

According to the data in Table 1,[36,62-66] ramie, sisal and buriti fibers had higher quantities of lignin, which may contribute to the formation of several intramolecular hydrogen bonds between neighboring phenolic groups in lignin. Such bonding reduces the distance between the neighboring phenolic groups, as can be seen by the lower hydrogen bond distance values for these fibers, compared to those for other fibers.

The hydrogen bond energy values for the bands at 3423 cm^{-1} and 3342 cm^{-1} are similar for all the fibers studied. However, considering these two bands in buriti fiber, it may be noted that they reach higher values, which may indicate a higher number of intra-molecular hydrogen bonds in cellulose in this fiber. These higher values were attributed to lower hydrogen bond distances, which may contribute to higher interactions between intra-molecular cellulose chains. The energy values at 3278 cm^{-1} and 3221 cm^{-1} are related to the cellulose allomorph forms for all the fibers studied.[53,56]

The energy of the hydrogen bonds and hydrogen bond distances for the varieties of fibers studied[5] are given in Table 2. Curaua, jute and kenaf fibers present a lower energy of hydrogen bonds at 3567 cm^{-1}. This could be associated with a higher quantity of absorbed water in the structure of these fibers, since the band at 3567 cm^{-1} is also assigned to the weakly absorbed water.[48,52]

The experimental X-ray diffraction profile between $s_o + s_o/2$ was matched with the simulated profile using Equations (1), (2), (3), (6) and (8), for various values of <N>, g, α and a parameter for background correction, so as to minimize the difference between them. For this purpose, a minimization algorithm SIMPLEX, which is a multidimensional program, was used.[54] Initial <N> the crystal size, g and the width of crystal distribution function values were determined using a well-established procedure.[33] The obtained microstructural parameters for the investigated vegetal fibers, using different Bragg reflections, are given in Table 3.

Figures 3 (a-f) and 4 (a-f) show the goodness of the fit between the simulated and the experimental intensity profiles for (110) and (200) prominent reflections, which is less than 10% of the mean value. Here, we compute:

$$\Delta^2 = \left[I_{cal} - \left(I_{exp} + BG \right) \right]^2 / \text{number of points} \qquad (8)$$

We also observe from these calculations that the exponential distribution function gives a better fit in these vegetal fibers and their native cellulose. It is evident from Table 3 that the strains present in these natural vegetal fibers and their native cellulose are very small and varies between 0.1% and 1.5%, when compared to polymer fibers.[55]

Figure 5 (a, b) shows the variations in the crystal size distribution along (110) and (200) for the vegetal fibers and their native cellulose.[57] The significant variation of <N> crystal size and lattice strain g is illustrated in Table 3. We have computed surface and volume weighted crystal sizes and we find that they are different in different directions, indicating that the shape of the crystallite is not spherical, but ellipsoid. There is also a significant variation of these microcrystalline parameters among the different types of vegetal fibers and their native cellulose. The reason for such a variation, even though these are made up of same chemical units, lies in the fact that the numbers of weak inter- and intramolecular hydrogen bonds, such as C=O, C-H, C-O-C and C-O, which determine the extent of ordering in the vegetal fibers and their native cellulose, vary significantly. In fact, there is a direct relation between the size and the shape of the crystallites with the number of hydrogen bonds in these fibers. For a better perspective of the results obtained for these fibers, we have projected the crystallite shape into a plane using the equation:

$$\left(\frac{2}{D_{hkl}} \right)^2 = \left(\frac{\cos \phi}{Y} \right)^2 + \left(\frac{\sin \phi}{X} \right)^2 \qquad (9)$$

where Φ is the angle between (hkl) planes. This Φ can be determined using the cell parameters reported here. The obtained crystallite shape is given in Figure 6.

It is evident from this figure that the volume of the ellipsoid shape in the varieties of vegetal fibers under study is comparatively higher than that of their native cellulose. As mentioned earlier, the weak intra- and intermolecular hydrogen bonds do play an important role in the extent of crystalline enthalpy, using Hosemann's relation $\alpha^* = g \times <N>^{1/2}$, which is an empirical parameter introduced by Hosemann. It essentially means that the growth of paracrystalline disorder is controlled by the net plane structure. Normally, for polymers the value of enthalpy lies between 0.1 and 0.2.

Table 2
Hydrogen bond distance and energy of the hydrogen bonds for the natural fibers studied

Fibers	3567 cm^{-1}		3423 cm^{-1}		3342 cm^{-1}		3278 cm^{-1}		3221 cm^{-1}	
	E_H (kJ)	R (Å)	E_H (kJ)	R (Å)	E_H (kJ)	R (Å)	E_H (kJ)	R (Å)	E_H (kJ)	R (Å)
Curaua	5.969	2.833	16.038	2.801	21.935	2.782	26.746	2.767	30.997	2.754
Jute	5.980	2.833	16.038	2.801	21.827	2.783	26.538	2.768	30.666	2.755
Kenaf	5.667	2.833	16.253	2.800	22.043	2.782	27.041	2.766	30.781	2.755
Ramie	6.048	2.832	16.325	2.800	22.100	2.782	26.782	2.767	31.140	2.754
Sisal	6.156	2.832	16.253	2.800	21.863	2.783	26.538	2.768	31.148	2.754
Buriti	6.185	2.832	16.253	2.800	22.366	2.781	27.041	2.766	31.184	2.753

Table 3
Microstructural parameters for the vegetal fibers studied and their native cellulose

| Fibers	Reflection	2θ (°)	<N>	P	α	g (%)	α*	d_{hkl} (Å)	D_{surf} (Å)	D_{vol} (Å)
Buriti	(100)	15.55	5.99±0.02	5.99	0.656	0.002±0.01	7.26	5.690	38.42	38.42
	(200)	22.00	8.09±0.05	3.18	0.315	1.07±0.02	6.80	4.035	36.58	39.98
Curaua	(100)	15.70	6.12±0.02	4.79	0.349	0.002±0.02	7.40	5.638	39.99	40.47
	(200)	22.20	12.56±0.07	12.43	0.255	2.57±0.02	8.74	4.00	47.76	50.13
Jute	(100)	15.30	1.78±0.01	0.08	0.477	0.92±0.02	10.44	5.784	32.73	33.98
	(200)	22.00	9.14±0.06	5.13	0.269	2.12±0.03	15.12	4.035	54.68	59.20
Kenaf	(100)	15.25	3.86±0.02	2.52	0.622	1.47±0.02	9.82	5.803	30.46	33.85
	(200)	22.00	8.06±0.04	5.27	0.291	2.57±0.03	14.20	4.035	41.64	43.98
Ramie	(100)	15.25	4.88±0.02	3.73	0.764	3.73±0.02	11.05	5.803	35.99	39.04
	(200)	22.10	6.81±0.03	3.71	0.301	1.83±0.02	13.05	4.017	39.39	42.67
Sisal	(100)	15.80	7.42±0.05	5.97	0.259	0.005±0.03	13.62	5.602	46.48	47.95
	(200)	21.85	5.41±0.02	3.44	0.328	1.74±0.02	11.63	4.081	35.22	38.69
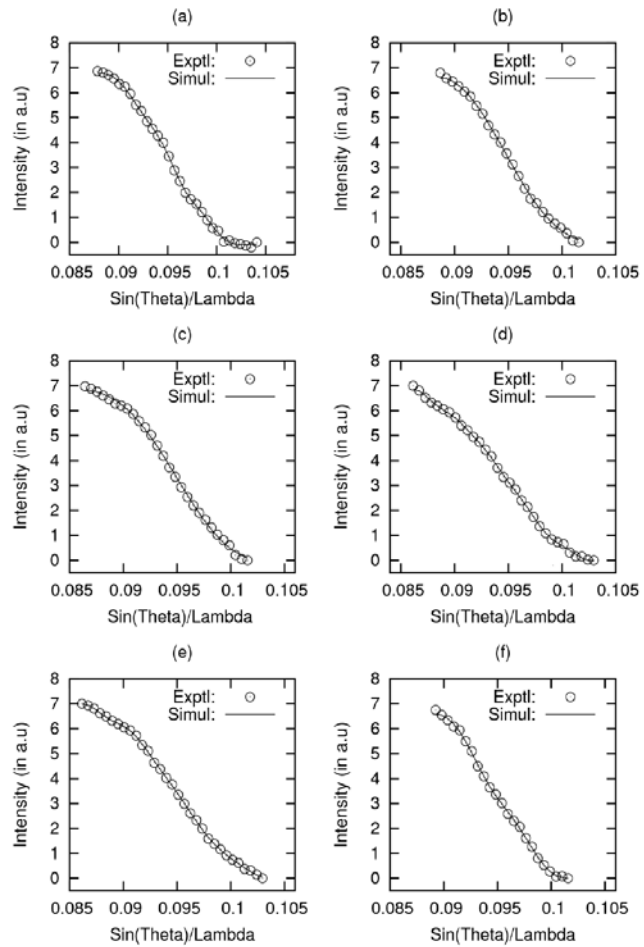
Figure 3: Experimental and simulated (110) reflection profile of a) buriti,
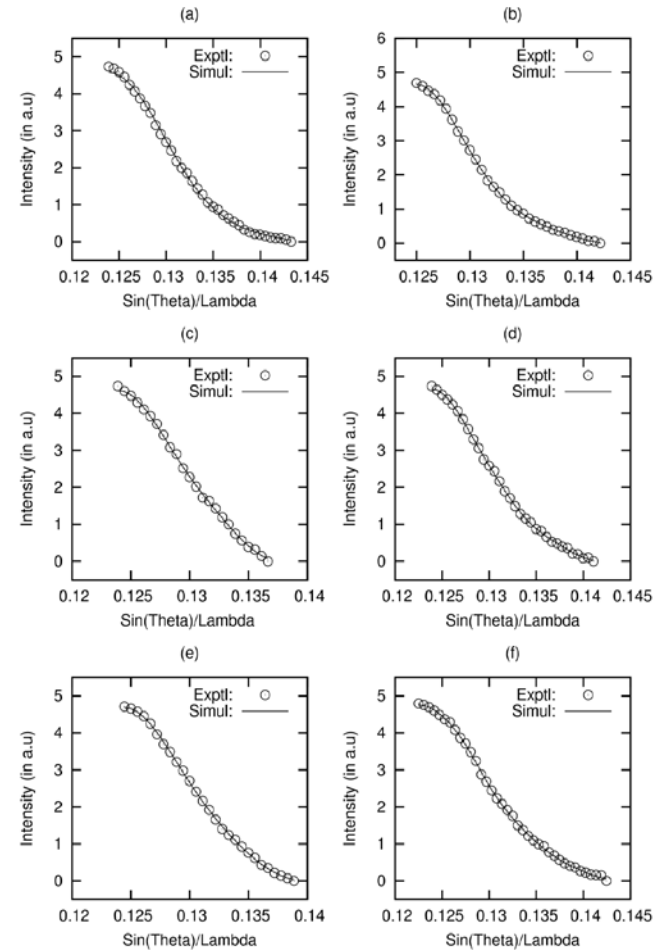b) curaua, c) jute, d) kenaf, e) ramie and f) sisal vegetal fibers

Figure 4: Experimental and simulated (200) reflection profile of a) buriti,
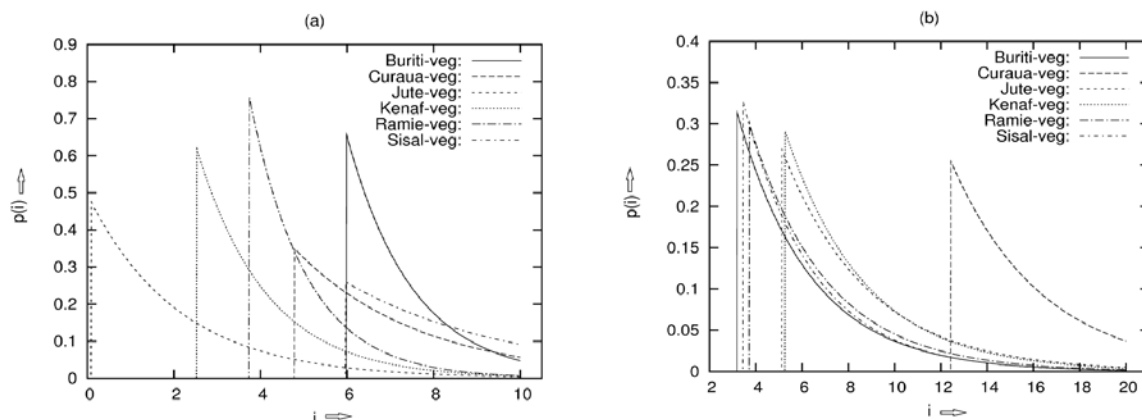b) curaua, c) jute, d) kenaf, e) ramie and f) sisal vegetal fibers

Figure 5: Variation of crystal size distribution along a) (110) and b) (200) reflection for buriti, curaua, jute, kenaf, ramie and sisal vegetal fibers
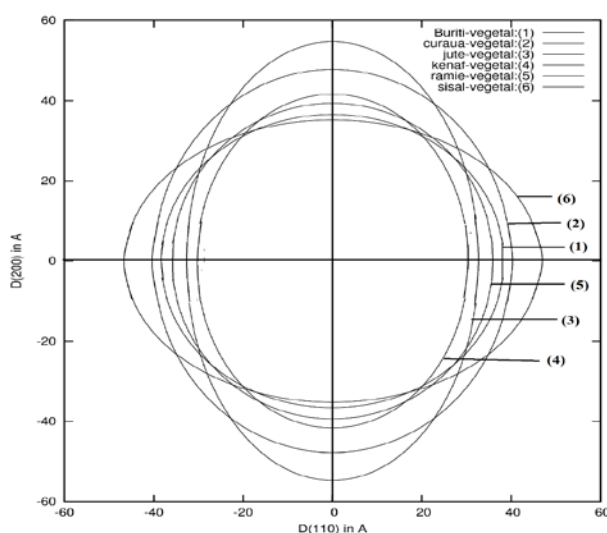

Figure 6: Variation of crystallite ellipsoid shape for (1) buriti, (2) curaua, (3) jute, (4) kenaf, (5) ramie and (6) sisal vegetal fibers

In the vegetal fibers and their native cellulose in this work, we find the value being less than 0.2. This may be explained by the fact that the strains present in the vegetal fibers and their native cellulose are very small, compared to other natural fibers, such as silk, and also man-made polymers.[58,59] The crystallite shape is different in the studied varieties of vegetal fibers and their native cellulose, compared to other fibers.[60]

There is a variation of crystallite shape and size for vegetal fibers and their native cellulose caused by variation in the chemical composition of cellulose and lignin, present among fibers.[36] Thus, the vegetal fibers and their native cellulose investigated in this work have larger values of crystallite shape and size. This finding is in agreement with an earlier report on man-made fibers.[61]

CONCLUSION

We have carried out FT-IR spectroscopy and X-ray diffraction analyses on a variety of vegetal fibers and their native cellulose. It is observed that, even though there is not much change in the position of the X-ray reflections, a significant difference in microstructural parameters occurs for the vegetal fibers and their native cellulose. The changes in crystal imperfection parameters are quantified here in terms of microstructural parameters and chemical composition of cellulose and lignin. Also, as revealed by FT-IR spectroscopy, a strong broad band can be observed in the region of 3700-3000 cm^{-1}, which is assigned to different –OH stretching modes.[19] The intermolecular hydrogen bond in the phenolic group of lignin was recorded around 3568-3577 cm^{-1}.[19] In cellulose, the hydrogen bond vibration

appears around 3432 cm^{-1},[36,48] while another intermolecular hydrogen bond in cellulose normally occurs at 3342 cm^{-1}.[48] These two significant characteristic bands assigned to the two crystalline cellulose allomorphs, cellulose I$_\alpha$ and cellulose I$_\beta$, also occur in the region of 3220-3280 cm^{-1}.[41,42] Our study indicated that the investigated vegetal fibers and their native cellulose have larger values of crystallite shape and size. Surprisingly, we observed that the strains present in the vegetal fibers and their native cellulose are very small. Thus, by the methods used here, our study provides deeper understanding of the structure and properties of vegetable fibers, which is necessary before exploring their potential as reinforcing fillers in composite formulations.

REFERENCES

[1] Y. Chen, M. A. Tshabalala, J. Gao, N. M. Stark, Y. Fan *et al*., *Thermochim. Acta*, **591**, 40 (2014), https://doi.org/10.1016/j.tca.2014.06.012

[2] S. Sheshmani, *Carbohyd. Polym*., **94**, 416 (2013), https://doi.org/10.1016/j.carbpol.2013.01.067

[3] C. Tenorio and R. Moya, *Thermochim. Acta*, **563**, 12 (2013), https://doi.org/10.1016/j.tca.2013.04.005

[4] G. Han, S. Huan, J. Han, Z. Zhang and Q. Wu, *Materials*, **7**, 16 (2014), https://doi.org/10.3390/ma7010016

[5] M. Poletto, A. J. Zattera and R. M. C. Santana, *J. Appl. Polym. Sci*., **126**, E337 (2012), https://doi.org/10.1002/app.36991

[6] H. L. Ornaghi Jr., M. P. Poletto, A. J. Zattera and S. C. Amico, *Cellulose*, **21**, 177 (2014), https://doi.org/10.1007/s10570-013-0094-1

[7] D. Romanzini, H. L. Ornaghi Jr., S. C. Amico and A. J. Zattera, *J. Reinf. Plast. Compos*., **31**, 1652 (2012), https://doi.org/10.1177/0731684412459982

[8] D. Klemm, B. Heublein, H. P. Fink and A. Bohn, *Angew. Chem. Int. Ed*., **44**, 3358 (2005), https://doi.org/10.1002/anie.200460587

[9] M. Åkerholm, B. Hinterstoisser and L. Salmén, *Carbohyd. Res*., **339**, 569 (2004), https://doi.org/10.1016/j.carres.2003.11.012

[10] S. Y. Oh, D. I. Yoo, Y. Shin, H. C. Kim, H. Y. Kim *et al*., *Carbohyd. Res*., **340**, 2376 (2005), https://doi.org/10.1016/j.carres.2005.08.007

[11] S. Nam, A. D. French, B. D. Condon and M. Concha, *Carbohyd. Polym*., **135**, 1 (2016), https://doi.org/10.1016/j.carbpol.2015.08.035

[12] R. J. Moon, A. Martin, J. Nairn, J. Simonsen and J. Youngblood, *Chem. Soc. Rev*., **40**, 3941 (2011), https://doi.org/10.1039/C0CS00108B

[13] P. Zugenmaier, *Pure Appl. Chem*., **78**, 1843 (2006), https://doi.org/10.1351/pac200678101843

[14] H. Hoogsteen, A. R. Postema, A. J. Pennings, G. T. Brinke and P. Zugenmaier, *Macromolecules*, **23**, 634 (1990), https://doi.org/10.1021/ma00204a041

[15] M. J. John and S. Thomas, *Carbohyd. Polym*., **71**, 343 (2008), https://doi.org/10.1016/j.carbpol.2007.05.040

[16] A. Gandini, *Green Chem*., **13**, 1061 (2011), https://doi.org/10.1039/C0GC00789G

[17] A. O'Sullivan, *Cellulose*, **4**, 173 (1997), https://doi.org/10.1023/A:1018431705579

[18] E. I. Hult, T. Iversen and J. Sugiyama, *Cellulose*, **10**, 103 (2003), https://doi.org/10.1023/A:1024080700873

[19] M. Poletto, V. Pistor and A. J. Zattera, in "Cellulose – Fundamental Aspects", edited by Theo van de Ven and Louis Godbout, IntechOpen, 2014, pp. 45-68, https://doi.org/10.5772/50452

[20] Y. Takahashi and H. Matsunaga, *Macromolecules*, **24**, 3968 (1991), https://doi.org/10.1021/ma00013a035

[21] U. J. Kim, S. H. Eom and M. Wada, *Polym. Degrad. Stabil*., **95**, 778 (2010), https://doi.org/10.1016/j.polymdegradstab.2010.02.009

[22] Y. Habibi, L. A. Lucia and O. J. Rojas, *Chem. Rev*., **110**, 3479 (2010), https://doi.org/10.1021/cr900339w

[23] H. L. Ornaghi Jr., A. S. Bolner, R. Fiorio, A. J. Zattera and S. C. Amico, *J. Appl. Polym. Sci*., **118**, 887 (2010), https://doi.org/10.1002/app.32388

[24] B. E. Warren and B. L. Averbach, *J. Appl. Phys*., **21**, 595 (1950), https://doi.org/10.1063/1.1699713

[25] B. E. Warren, *Acta Cryst*., **8**, 483 (1955), https://doi.org/10.1107/S0365110X55001503

[26] B. E. Warren, "X-Ray Diffraction", New York, Addison-Wesley, 1969.

[27] H. P. Fink, D. Hofmann and B. Philipp, *Cellulose*, **2**, 51 (1995), https://doi.org/10.1007/BF00812772

[28] J. Haase and B. Renwanz, *Kolloid-Z. Z. Polym*., **250**, 503 (1972), https://doi.org/10.1007/BF01521246

[29] J. Haase, R. Hosemann and B. Renwanz, *Kolloid-Z. Z. Polym*., **251**, 871 (1973), https://doi.org/10.1007/BF01520918

[30] J. Haase, R. Hosemann and B. Renwanz, *Cellulose Chem. Technol*., **9**, 513 (1975), http://www.cellulosechemtechnol.ro/

[31] D. Hofmann and E. Walenta, *Polymer*, **28**, 1271 (1987), https://doi.org/10.1016/0032-3861(87)90436-8

[32] D. Hofmann, H. P. Fink and B. Philipp, *Polymer*, **30**, 237 (1989), https://doi.org/10.1016/0032-3861(89)90111-0

[33] I. H. Hall and R. Somashekar, *J. Appl. Cryst.*, **24**, 1051 (1991), https://doi.org/10.1107/S0021889891007707

[34] R. Somashekar and H. Somashekarappa, *J. Appl. Cryst.*, **30**, 147 (1997), https://doi.org/10.1107/S0021889896010023

[35] R. Somashekar, H. Somashekarappa, G. Subramanyam and U. D. Prahllad, *Eur. Polym. J.*, **33**, 963 (1997), https://doi.org/10.1016/S0014-3057(96)00149-8

[36] M. Poletto, H. L. Ornaghi Jr. and A. J. Zattera, *Materials*, **7**, 6105 (2014), https://doi.org/10.3390/ma7096105

[37] A. D. French and M. S. Cintrón, *Cellulose*, **20**, 583 (2013), http://dx.doi.org/10.1007/s10570-012-9833-y

[38] R. A Young, R. J. Gerdes and A. J. C. Wilson, *Acta Cryst.*, **22**, 155 (1967), https://doi.org/10.1107/S0365110X67000271

[39] R. Somashekar, I. H. Hall and P. D. Carr, *J. Appl. Cryst.*, **22**, 363 (1989), https://doi.org/10.1107/S0021889889004085

[40] I. H. Hall and R. Somashekar, *J. Appl. Cryst.*, **24**, 1051 (1989), https://doi.org/10.1107/S0021889891007707

[41] H. Yang, R. Yan, H. Chen, D. H. Lee and C. Zheng, *Fuel*, **86**, 1781 (2007), https://doi.org/10.1016/j.fuel.2006.12.013

[42] C. M. Popescu, G. Singurel, M. C. Popescu, C. Vasile, D. S. Argyropoulos *et al.*, *Carbohyd. Polym.*, **77**, 851 (2009), https://doi.org/10.1016/j.carbpol.2009.03.011

[43] H. Yokoi, T. Nakase, K. Goto, Y. Ishida, H. Ohtani *et al.*, *J. Anal. Appl. Pyrol.*, **67**, 191 (2003), https://doi.org/10.1016/S0165-2370(02)00061-X

[44] Y. Ishida, K. Goto, H. Yokoi, S. Tsuge, H. Ohtani *et al.*, *J. Anal. Appl. Pyrol.*, **78**, 200 (2007), https://doi.org/10.1016/j.jaap.2006.06.009

[45] E. Mészáros, E. Jakab and G. Várhegyi, *J. Anal. Appl. Pyrol.*, **79**, 61 (2007), https://doi.org/10.1016/j.jaap.2006.12.007

[46] M. C. Popescu, C. M. Popescu, G. Lisa and Y. Sakata, *J. Mol. Struct.*, **988**, 65 (2011), https://doi.org/10.1016/j.molstruc.2010.12.004

[47] I. Carrilo, R. T. Mendonça, M. Ago and O. J. Rojas, *Cellulose*, **25**, 1011 (2018). https://doi.org/10.1007%2Fs10570-018-1653-2

[48] T. Kondo, *Cellulose*, **4**, 281 (1997), https://doi.org/10.1023/A:1018448109214

[49] C. M. Popescu, M. C. Popescu and C. Vasile, *Carbohyd. Polym.*, **79**, 362 (2010), https://doi.org/10.1016/j.carbpol.2009.08.015

[50] H. Struszczyk, *J. Macromol. Sci.*, **23**, 973 (1986), https://doi.org/10.1080/00222338608081105

[51] G. C. Pimentel and C. H. Sederholm, *J. Chem. Phys.*, **24**, 639 (1956), https://doi.org/10.1063/1.1742588

[52] C. M. Popescu, M. C. Popescu, G. Singurel, C. Vasile, D. S. Argyropoulos *et al.*, *Appl. Spectrosc.*, **61**, 1168 (2007), https://doi.org/10.1366/000370207782597076

[53] M. Poletto, M. Zeni and A. J. Zattera, *J. Thermoplast. Compos. Mater.*, **25**, 821 (2012), https://doi.org/10.1177/0892705711413627

[54] W. Press, B. P. Flannery, S. Teuklosky and W. T. Vettering, "Numerical Recipes", New York, Cambridge University Press, 1988, p. 284

[55] S. Abhishek, O. M. Samir, V. Annadurai, R. Gopalkrishne Urs, S. S. Mahesh *et al.*, *Eur. Polym. J.*, **41**, 2916 (2005), https://doi.org/10.1016/j.eurpolymj.2005.06.005

[56] Sangappa, B. Lakshmeesha Rao, S. Asha, R. Madhu Kumar *et al.*, *Compos. Interfaces*, **21**, 153 (2014), https://doi.org/10.1080/15685543.2013.855485

[57] H. Somashekarappa, V. Annadurai, Sangappa, G. Subramanya and R. Somashekar, *Materials Letters*, **53**, 415 (2002), https://doi.org/10.1016/S0167-577X(01)00517-1

[58] R. Hosemann, *Colloid. Polym. Sci.*, **260**, 864 (1982), https://doi.org/10.1007/BF01419097

[59] V. Annadurai, G. Subramanyam, R. Goplakrishne Urs and R. Somashekar, *J. Appl. Polym. Sci.*, **79**, 1979 (2001), https://doi.org/10.1002/1097-4628(20010314)79:11<1979::AID-APP1005>3.0.CO;2-Y

[60] K. Ranjitha, G. Gayathri, R. Tomar, M. Poletto, V. Annadurai *et al.*, *AIP Conf. Procs.*, **1859**, 020054 (2017), https://doi.org/10.1063/1.4990207

[61] K. G. Lee, R. Barton Jr. and J. M. Schultz, *J. Polym. Sci. (Part B)*, **33**, 1 (1995), https://doi.org/10.1002/polb.1995.090330101

[62] O. Faruk, A. K. Bledzki, H. Fink and M. Sain, *Prog. Polym. Sci.*, **37**, 1552 (2012), https://doi.org/10.1016/j.progpolymsci.2012.04.003

[63] A. K. Bledzki and J. Gassan, *Prog. Polym. Sci.*, **24**, 221 (1999), https://doi.org/10.1016/S0079-6700(98)00018-5

[64] N. C. Cordeiro, A. G. O. Gouveia, A. M. Moraes and S. C. Amico, *Carbohyd. Polym.*, **84**, 110 (2011), https://doi.org/10.1016/j.carbpol.2010.11.008

[65] K. G. Satyanarayana, J. L. Guimarães and F. Wypych, *Compos. Part A*, **38**, 1694 (2007), https://doi.org/10.1016/j.compositesa.2007.02.006

[66] H. L. Ornaghi Júnior, A. G. O. Moraes, M. Poletto, A. J. Zattera and S. C. Amico, *Cellulose Chem. Technol.*, **50**, 15 (2016), http://www.cellulosechemtechnol.ro/pdf/CCT1(2016)/p.15-22.pdf